

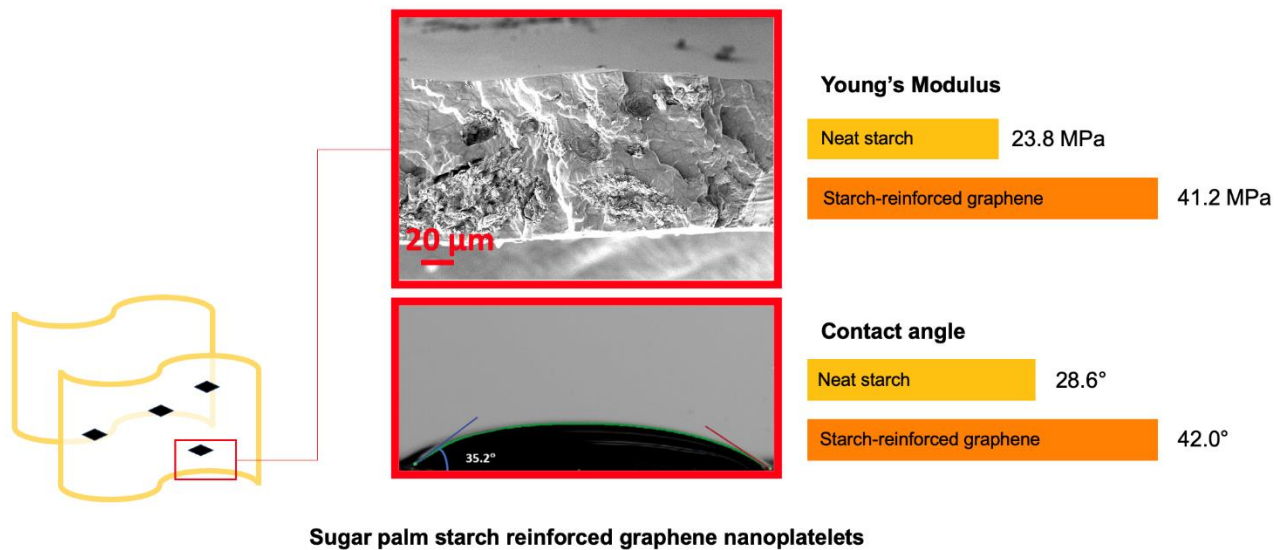
Thermoplastic Sugar Palm Starch Reinforced Graphene Nanoplatelets for Sustainable Biocomposite Films

Noor Fadhilah Rahmat,^{a,b,c} Mohd Shaiful Sajab,^{a,b,*} Atiqah Mohd Afdzaluddin,^d Gongtao Ding,^e and Chin Hua Chia^f

*Corresponding author: mohdshaiful@ukm.edu.my

DOI: 10.15376/biores.19.1.1526-1541

GRAPHICAL ABSTRACT



Thermoplastic Sugar Palm Starch Reinforced Graphene Nanoplatelets for Sustainable Biocomposite Films

Noor Fadhilah Rahmat,^{a,b,c} Mohd Shaiful Sajab,^{a,b,*} Atiqah Mohd Afdzaluddin,^d Gongtao Ding,^e and Chin Hua Chia^f

Graphene nanoplatelets (GNP) were incorporated into thermoplastic starch (TPS) films, and effects on water absorption and mechanical properties were investigated. GNP inclusion formed a barrier that significantly reduced water absorption, resulting in denser TPS/GNP films. Fourier-transform infrared spectroscopy (FTIR) revealed changes in chemical interactions, and FESEM analysis showed improved GNP dispersion at this concentration. Water contact angle results indicated increased hydrophobicity with higher GNP content. Positive influences on mechanical properties, such as tensile strength and Young's modulus, were observed at 12 wt% GNP, but excessive GNP content caused agglomeration and reduced ductility. The study results highlight the potential of GNP-reinforced TPS films for improved water resistance and mechanical properties, emphasizing the need for careful optimization in future research.

DOI: 10.15376/biores.19.1.1526-1541

Keywords: Biocomposite; Graphene; Sustainable packaging; Starch

Contact information: a: Research Center for Sustainable Process Technology (CESPRO), Faculty of Engineering and Built Environment, Universiti Kebangsaan Malaysia, 43600 Bangi, Selangor, Malaysia; b: Department of Chemical and Process Engineering, Faculty of Engineering and Built Environment, Universiti Kebangsaan Malaysia, 43600 Bangi, Selangor, Malaysia; c: Department of Physics, Centre for Defence Foundation Studies, Universiti Pertahanan Nasional Malaysia, 57000 Kuala Lumpur, Malaysia; d: Institute of Microengineering and Nanoelectronics, Universiti Kebangsaan Malaysia, 43600 UKM Bangi, Selangor, Malaysia; e: Key Laboratory of Biotechnology and Bioengineering of State Ethnic Affairs Commission, Biomedical Research Center, Northwest Minzu University, Lanzhou 730030, PR China; f: Materials Science Program, Faculty of Science and Technology, Universiti Kebangsaan Malaysia, Bangi, Malaysia; *Corresponding author: mohdshaiful@ukm.edu.my

INTRODUCTION

Currently, renewable and biodegradable biopolymers have attracted considerable interest as promising green materials in a variety of applications, including intelligent food packaging, biomedical, membranes, and automotive. Their sustainability, biodegradability, and use of eco-friendly methods are crucial for the future of packaging materials (Cataldi *et al.* 2018; Chia *et al.* 2023). Starch, as the second most important renewable source after cellulose, stands out as an abundant and biodegradable polysaccharide (Cheng *et al.* 2021). It has been a key ingredient in food applications, offering sweetness, thickness, binding, and emulsifying properties (Yemenicioğlu *et al.* 2020). Thermoplastic starch (TPS) is a biodegradable polymer and derived from natural starch. It is extracted from sources such as corn, wheat, and potato. It can be processed using conventional thermoplastic processing techniques, making it a versatile material for various applications (Bumrungrnok *et al.* 2023).

However, the TPS and other biodegradable composites face challenges including a highly hydrophilic nature, poor mechanical capabilities, and insufficient thermal stability for various applications, such as intelligent food packaging, biomedical, membranes, and automotive. Researchers aim to enhance the properties of TPS and biodegradable composites, striving to create innovative composite materials that can overcome existing limitations (Vinod *et al.* 2020; George *et al.* 2020; Arpitha *et al.* 2022). Additionally, it has some limitations in terms of its mechanical and barrier properties. Thus, researchers are exploring starch modification techniques to improve its properties and develop novel composites. The addition of nanofillers to TPS can be an effective way to tailor its properties for specific applications (Chen *et al.* 2020). There are different types of nanofillers that can be used to enhance the properties of TPS, including cellulose nanofibers, nanoclays, and carbon (Shahbazi *et al.* 2017).

Graphene, a two-dimensional structure consisting of sp^2 -bonded carbon atoms, has been regarded as one of the most effective nanofillers for the modification of other materials. The addition of graphene nanoplatelets (GNP) is expected to improve the stiffness, strength, thermal tolerance, and electrical conductivity of TPS, making it suitable for a wider range of applications (Mohan *et al.* 2021a; Khalid *et al.* 2022; Namdev *et al.* 2023). Incorporating GNP is one of the cost-effective carbon materials that possess the unique ability to transform the mechanical properties of polymers. GNP possess exceptional mechanical properties, such as high tensile strength and flexibility. This can make biofilms more robust and durable, allowing for applications in areas where strength is crucial, such as in packaging materials or coatings (Scaffaro *et al.* 2017). GNP has a high gas barrier property, which can improve the shelf life of food packaging made from thermoplastic starch. It also has interesting properties such as being light, having a high aspect ratio, being electrically and thermally conductive, being tough, costing little, and having a flat structure (Cataldi *et al.* 2018). Furthermore, GNP can also interact with water molecules through van der Waals forces, which can further reduce the amount of available water that can penetrate the matrix.

The aim of this research was to fabricate biocomposite films using sugar palm starch as the base material. Because TPS has the ability to use water as a universal solvent, it can facilitate the even distribution of GNP nanoparticles within the polymer matrix. Therefore, this study examines the influence of GNP nanoparticles on the morphological and mechanical characteristics at different concentrations.

EXPERIMENTAL

Materials

The TPS was prepared from sugar palm tree at Jempol, Negeri Sembilan, Malaysia. The GNP nanoparticles in powder form (particle size of $< 2 \mu\text{m}$, the thickness of few nm, and surface area of $300 \text{ m}^2/\text{g}$) and glycerol ($\geq 99.0\%$) were procured from Sigma Aldrich, Darmstadt, Germany.

Fabrication of TPS/GNP Film

Briefly, solution was prepared by combining 7.0 g of powdered sugar palm starch with glycerol plasticizer at a ratio of 30% w/w starch basis. This mixture was then dissolved in 180 mL of distilled water. The TPS with various concentration of GNP nanoparticles (0.75, 1.5, 3, 6, 12, and 15 wt%) was agitated using a magnetic stirrer at 1,000 rpm and a

temperature at 90 °C for a duration of 50 min. Subsequently, the prepared TPS/GNP composites were homogenized using the Ultra-Turrax T25 digital homogenizer (Janke & Kunkel, IKA-Labortechnik, Staufen, Germany) at a speed of 10,000 rpm for 10 min.

Both TPS and TPS/GNP films were fabricated *via* the solution casting technique. To initiate proper drying, 80 mL of the sample was cast onto designated plates and dried in an oven at 105 °C for 24 h. The resulting films, ranging from 0.1 to 0.3 mm in thickness, were delicately peeled off from the plates and stored under ambient conditions (25 ± 2 °C and 55 ± 1% relative humidity (RH)) to prevent any moisture absorption.

Density and Swelling Ratio

The water absorption test was performed using ASTM D570-98 (1998). Initially, the film samples were dried for 24 h at a temperature of 105 °C, and their weights were recorded in grams, M_0 . Subsequently, the samples were immersed in deionized water at room temperature, and the weight gain of the specimens was measured as a function of time after removing any water present on their surfaces, M_t . The difference between the initial and final masses was determined by applying Eq. 1:

$$\text{Water absorption (\%)} = \frac{(M_t - M_0)}{M_0} \quad (1)$$

Samples were determined utilizing Electronic Densimeter MD-3005, and ASTM D792-00 (2000). The preliminary dry matter of each sample was determined. The film samples were weighed (m) before being immersed into the liquid of volume (V) solvent. The sample's density (ρ) was calculated using Eq. 2:

$$\rho = m/V \quad (2)$$

The quantity of GNPs incorporated into the matrix directly affects the film's density. In addition, to evaluate the density of GNP content, seven conditions with 0 to 15 wt% GNPs were tested three times for each sample and the average value was measured.

Characterization

Contact angle measurements for the film surface characterization were performed with the Ossila Contact Angle Goniometer (L2004A1) (Ossila BV, Leiden, Netherlands) equipped with a digital camera (CCD). The contact angle of the films was estimated by the sessile drop method, whereby, a droplet of distilled water (10 µL) was deposited on the surface of 1.5 cm x 1.5 cm films using an automatic piston pipette. The digital camera was placed horizontally to capture the drop image. An image analyzer software (Profile Analysis Tensiometer PAT-1, (Sinterface, Berlin, Germany) was used to measure the angle formed between the surface of the film in contact with the drop and the tangent to the drop of liquid at the point of contact with the film surface. Both film surfaces were tested, and five measurements were performed on each side of the film.

The functional group of the all samples were determined using attenuated total reflectance Fourier transform infrared, ATR-FTIR (ALPHA FTIR Spectrometer, Bruker, Billerica, MA, USA) in the range of 4000 to 500 cm^{-1} at a resolution of 1 cm^{-1} . The effect of incorporation of nanofiller on the mechanical properties of starch nanocomposites was analyzed by tensile strength, Young's modulus, and elongation at break from the stress-strain data conducted using Instron® Electromechanical Universal Testing Systems 3300 Series with a load cell of 1 kN with a grip distance of 50 mm and a crosshead speed of 5 mm/min at room temperature. Each sample included five tested replicates to obtain a

reliable mean and standard deviation. According to the test, tensile stress, strain, elongation at break, and Young's modulus were determined.

The morphology of all the materials, including neat graphene nanoplatelets, neat sugar palm starch, TPS/GNP film and the morphological structure of fractured films was observed by field emission scanning electron microscope (FESEM) (Merlin Compact, Zeiss Pvt Ltd., Oberkochen, Germany). The samples were mounted on an aluminum sample mount before being sputtered with iridium sputter coater (Quorum, East Sussex, United Kingdom) to prevent charging.

RESULTS AND DISCUSSION

Water Diffusion

To identify the effect of GNP nanoparticles on the water diffusion of the prepared sample, an analysis of water uptake kinetics was performed and analyzed according to the Fick's transition equation below (Muthukumar *et al.* 2022),

$$\frac{\partial C}{\partial t} = D \left(\frac{\partial^2 C}{\partial x^2} \right) \quad (3)$$

where C is the water concentration mg/m^3 , t is a time (min), x is the distance into the thickness sample (m), and D is the diffusion coefficient (m^2/min). The diffusion coefficient can be described based on the Fick's second law, where $\frac{M_t}{M_\infty} \leq 0.6$ can be reduced to:

$$\frac{M_t}{M_\infty} = \frac{4}{\pi^{1/2}} \left(\frac{Dt}{h^2} \right)^{1/2} \quad (4)$$

For $\frac{M_t}{M_\infty} > 0.6$, the equation can be reduced to,

$$\frac{M_t}{M_\infty} = 1 - \exp \left[-7.3 \left(\frac{Dt}{h^2} \right)^{0.75} \right] \quad (5)$$

where M_t and M_∞ are the water uptake at the time t and equilibrium. The influence of GNP nanoparticles at concentrations of 0, 0.75, and 12 wt% is depicted in Fig. 1 and fitted based on the Fick's second law of diffusion and the data is tabulated in Table 1.

The graph indicates that, initially, the water uptake rate was rapid, followed by a gradual increase until reaching equilibrium state. The neat TPS layer exhibited the highest water absorption, as TPS possesses strong hydrophilicity, making it prone to notable water absorption compared to other composites. However, water absorption drastically decreased with increased GNP content. The incorporation of GNP nanoparticles demonstrates an effective reduction in water absorption of the TPS/GNP films.

This can be attributed to the barrier formation by GNP nanoparticles, which hinders water penetration into the TPS matrix. Graphene nanoplatelets possess hydrophobic properties, rendering them highly impermeable to water (Namdev *et al.* 2023). The introduction of GNP into the TPS matrix forms a network structure that restricts the availability of free space for water molecules to permeate the matrix. Consequently, the water absorption capacity of the starch matrix is reduced. The incorporation of GNP creates a barrier that limits the penetration of water, thereby mitigating the moisture uptake by the TPS material. Incorporating GNP nanoparticles resulted in a substantial enhancement of the coefficient of diffusion, D , according to Fick's law, reaching $3.12 \times 10^{-6} \text{ cm}^2 \cdot \text{s}^{-1}$.

The density of the films can contribute to understanding the water diffusion process. The density of the TPS films at varying GNP loadings is given in Table 1. All the TPS/GNP films showed higher density relative to the TPS based film. As can be seen, the TPS with the 0.75 wt% of GNP had the lowest density, with value 1.27 g/cm³. The increase in density was directly attributed to the density of GNP nanoparticles, which was 2.21 g/cm³ at a temperature of 25 °C. This indicates that as the density of the nanoparticles increased, the overall density of the TPS/GNP films also increased up to 1.61 g/cm³. It is possible that because GNP nanoparticles served as a nanofiller, it reduced the void spacing between the starch particles, resulting in a denser film (Ahmad *et al.* 2015).

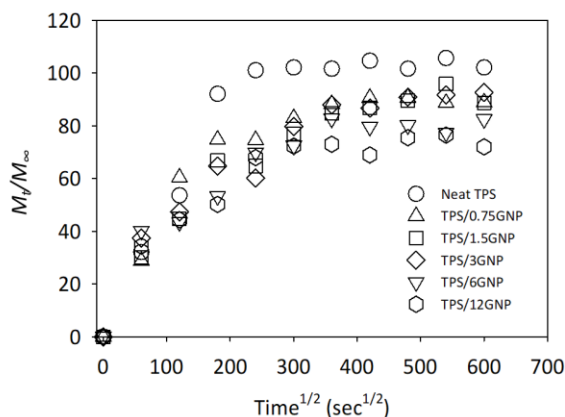


Fig. 1. Water absorption uptake of TPS and TPS biocomposites films at room temperature

Table 1. Diffusion and Density of TPS and TPS Biocomposites Films in the Addition of GNP Nanoparticles

Films	Fick's Law Coefficient of Diffusion, D ($\times 10^{-6} \text{ cm}^2 \cdot \text{s}^{-1}$)	Density (g/cm ³)
Neat TPS	4.253	1.04
TPS/0.75GNP	4.158	1.33
TPS/1.5GNP	3.554	1.52
TPS/3GNP	3.423	1.40
TPS/6GNP	3.117	1.52
TPS/12GNP	3.982	1.47
TPS/15GNP	3.955	1.61

Chemical Characteristics

Fourier transform infrared (FTIR) spectroscopy was employed to investigate the chemical interactions and molecular structure of TPS films, as shown in Fig. 2. There was a wide band ranging from 3200 to 3300 cm⁻¹, which indicates a strong stretching of the O-H group, rendering the TPS film highly hydrophilic (Sohany *et al.* 2021; Bidari *et al.* 2023). This implies that the substance demonstrates a notable attraction towards water molecules. However, it is worth noting that the incorporation of 12 wt% GNP into the TPS film led to a substantial decrease in the observed bending of OH bonds, suggesting a potential impact on its water absorption capabilities (Mohan *et al.* 2022). Moreover, a distinctive band was identified between 1637 and 1647 cm⁻¹, indicating the bending of OH bonds of water molecules. This observation confirms the hygroscopic nature of thermoplastic starch, implying its ability to readily absorb and interact with water (John *et al.* 2020). Another

notable feature in the spectra is the absorbance peak found between 2924 and 2931 cm^{-1} , attributed to the C-H stretching vibration of the C-H methyl group (Nordin *et al.* 2020).

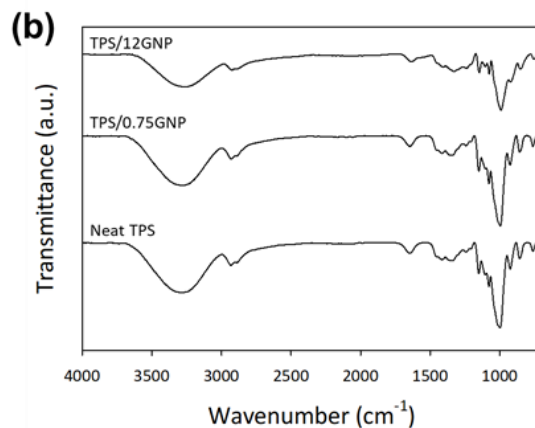


Fig. 2. FTIR spectrum of TPS and TPS biocomposites films with the addition of 0.75 and 12% GNP

Surface Morphology

To assess the dispersion of GNP nanoparticles within TPS films, the morphological structures of neat TPS, GNP, and reinforced biocomposite films of TPS/GNP were examined using FESEM (see Fig. 3). The GNP nanoparticles in Fig. 3(a) showed a distinct size ratio of the particles and short stacks of platelet-shaped graphene sheets. These layers are held together by van der Waals forces (Mohan *et al.* 2020a). Based on Fig. 2(b), the TPS had a smooth and clean fracture surface due to its brittle behavior at room temperature. In contrast, when 0.75 wt% of GNP was added to the starch matrix, voids were observed and the fracture surface condition became rougher. Furthermore, the FESEM analysis reveals the presence of clusters and agglomerations of GNP nanoparticles within the TPS/GNP films. These clusters can have an influence on the barrier properties and mechanical characteristics of the films. Among the TPS/GNP films, the specimen with a GNP concentration of 12 wt% demonstrated a more uniform dispersion of nanoparticles within the polymer matrix compared to the other formulation. This improved dispersion is believed to contribute to enhanced mechanical strength in the TPS/12GNP film.

In addition to micrograph of FESEM, surface roughness was assessed to characterize the properties of the films (see Fig. 4). The contact angle, which is a commonly used parameter to evaluate wettability and surface hydrophobicity, was employed in this study. High contact angles ($\theta > 90^\circ$) are indicative of a hydrophobic surface, while low contact angles ($\theta < 90^\circ$) are associated with hydrophilic surfaces (Kabir and Garg 2023; Otàlora González *et al.* 2020).

In line with the water uptake behavior observed in the TPS and TPS/GNP films, the water contact angle results displayed a similar trend. The addition of 0.75 wt% of GNP led to an increase in the water contact angle from 28.6° to 33.8°. Notably, the highest water contact angle of 42.0° was attained with a GNP content of 12 wt%. However, for the specimen with 15 wt% GNP, the water contact angle decreased. This decrease can be attributed to the poor dispersion of the high concentration of GNP within the film matrix, which affected the overall surface characteristics and hydrophobicity of the composite material. Due to its greater wettability compared to TPS/GNP, TPS demonstrates a correlation with contact angle, serving as an indicator of surface energy between the

polymer and graphene oxide. This relationship highlights the higher surface energy associated with polymers exhibiting increased wettability (Feng *et al.* 2023).

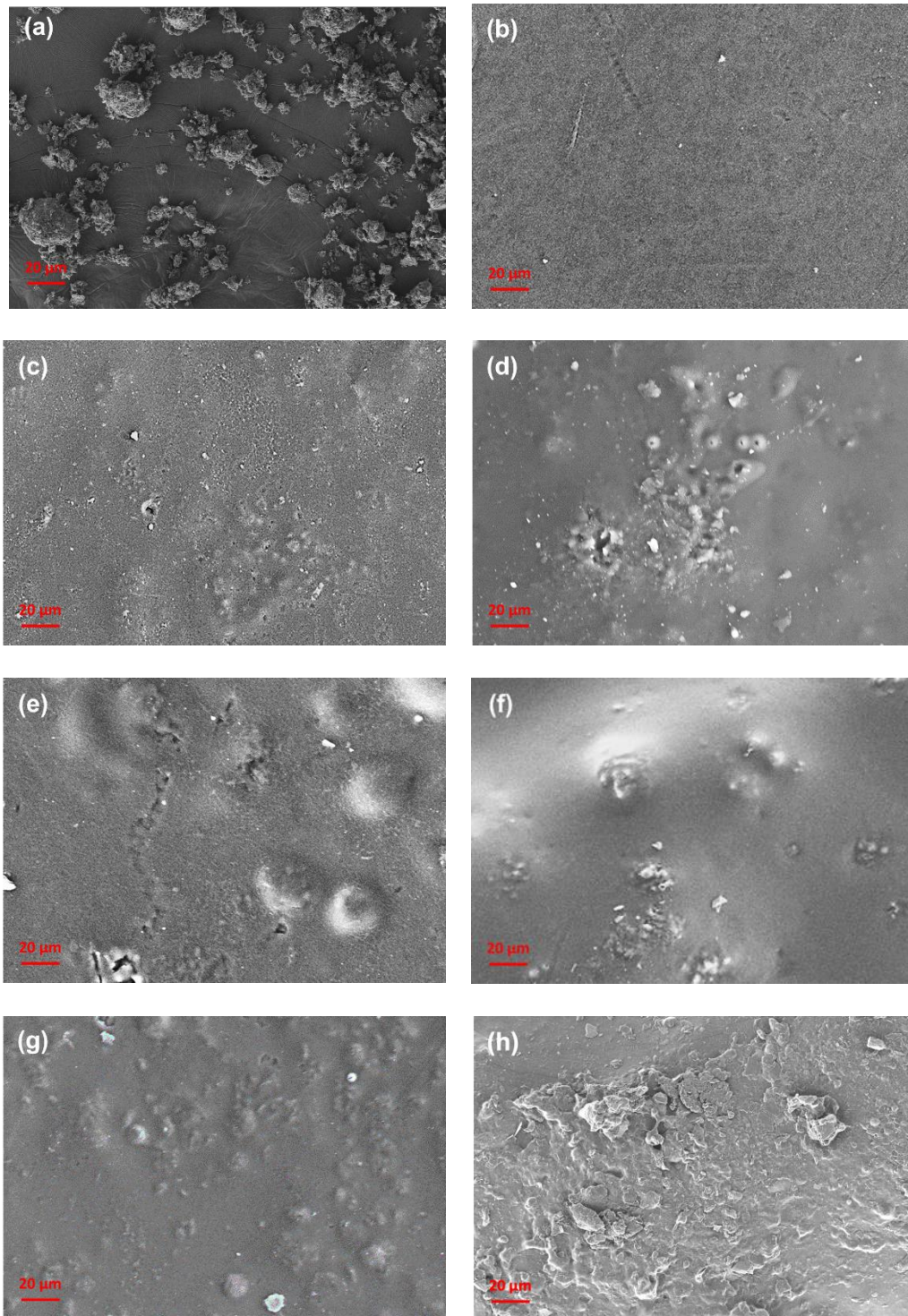


Fig. 3. FESEM micrograph of (a) GNP particles, (b) TPS, (c) TPS/0.75GNP, (d) TPS/1.5GNP, (e) TPS/3GNP, (f) TPS/6GNP, (g) TPS/12GNP, and (h) TPS/15GNP

The contact angle of the TPS film can be attributed to its nonporous, smooth surface with low surface roughness as in FESEM micrograph (see Fig. 2(b)). This observation aligns with previous studies indicating that the contact angle is influenced by capillary porosity and surface tension (Dong *et al.* 2021). As the GNP content increased in the composite films, the contact angle correspondingly increased, indicating increased hydrophobicity. This enhanced hydrophobicity can be attributed to two main factors: (a) the increased roughness has been observed in FESEM micrographs and (b) the inherent hydrophobic nature of GNP itself, which imparts greater hydrophobicity to the composite material (Tarhini and Tehrani-Bagha 2019; Kim *et al.* 2022).

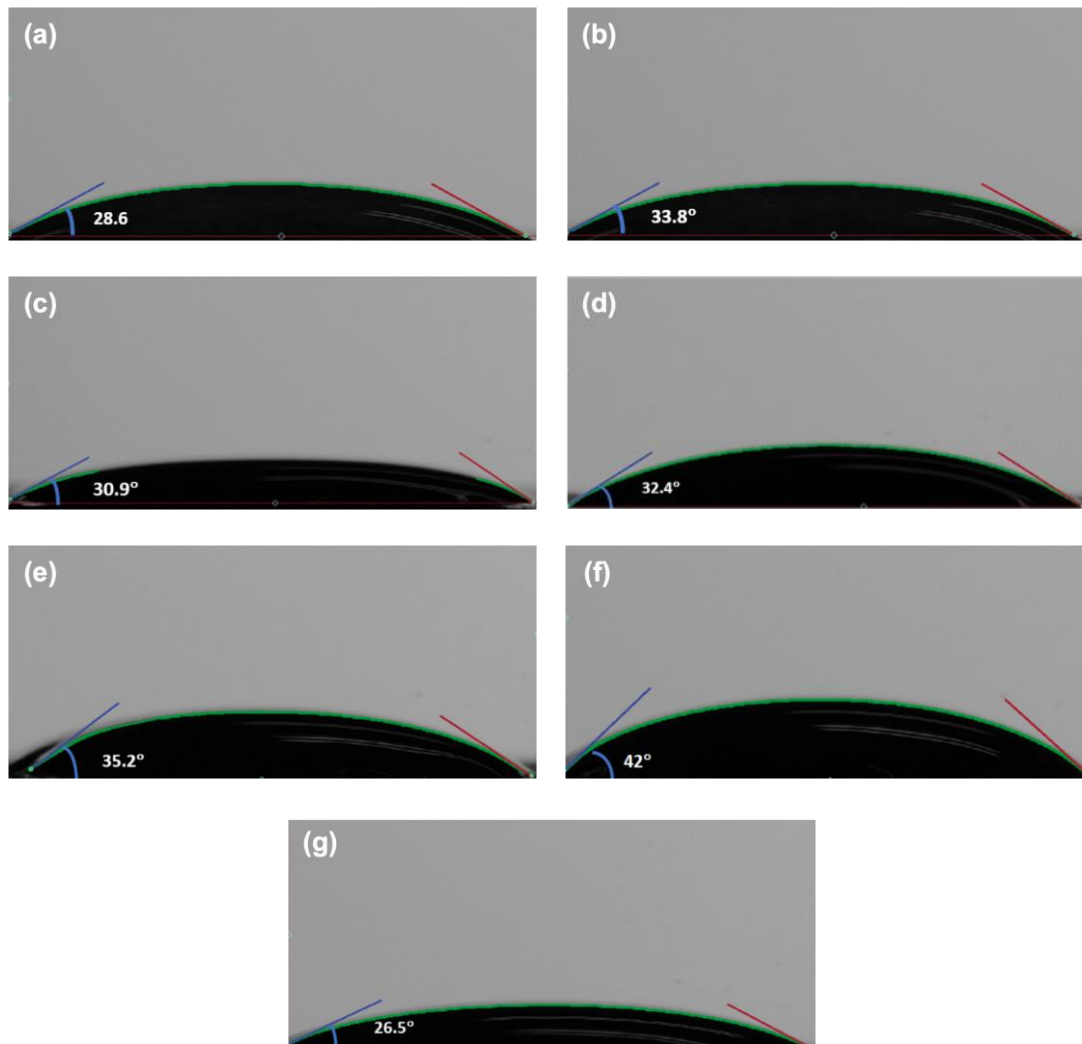


Fig. 4. The water contact angle of the biocomposites films of (a) TPS, (b) TPS/0.75GNP, (c) TPS/1.5GNP, (d) TPS/3GNP, (e) TPS/6GNP, (f) TPS/12GNP, and (g) TPS/15GNP

Mechanical Properties of TPS/GNP Films

Figure 5(a) illustrates the stress-strain behavior of the TPS films with different concentrations of GNP nanoparticles. Analyzing these curves, the trends of the tensile strength and Young's modulus are depicted to showcase the specific impact of GNP nanoparticles on these mechanical properties. The neat TPS film exhibited sufficient tensile strength, measuring at 1.39 MPa. This strength is primarily due to the presence of intermolecular bonds such as hydrogen bonds and van der Waals forces. The

intermolecular interactions between starch molecules are of the greatest importance as they effectively contribute to the overall structural integrity of the substance (Gutiérrez *et al.* 2018).

At low concentration of GNP nanoparticles, the particles can create a stable and uniform dispersion with starch molecules when distributed within the starch matrix. This is facilitated by good compatibility between the particles and starch molecules. Specifically, when the GNP content reached 12 wt%, it exhibited excellent compatibility with the starch matrix. Consequently, the composite with 12 wt% GNP demonstrated enhanced tensile strength compared to the other samples with varying GNP loadings. However, when the GNP content reached 15 wt% in the TPS matrix, the tensile strength decreased to 0.56 MPa. The high concentration of GNP nanoparticles led to their aggregation, which hindered their effective dispersion within the starch matrix. Additionally, aggregation plays a significant role in this process and these defects have the potential to grow larger than the critical crack size, ultimately leading to failure of the composite material.

Although the tensile strain decreased as the GNP nanoparticles content increased from 29.4 to 3.76%, the Young's modulus increased with the addition of GNP nanoparticles, indicating a stiffening effect (see Fig. 5(b)). The GNP nanoparticles acted as stress concentrators, distributing the applied force's energy more evenly throughout the material indicating that the GNP nanoparticles incorporated GNP into the nylon matrix increased Young's modulus by more than twice strengthened the starch matrix, making it less prone to deformation (Papadopoulou *et al.* 2016; Mergen *et al.* 2020; Kiziltas *et al.* 2021). When 0.75 wt% of GNP nanoparticles was added, the modulus increased from 23.8 to 30.4 MPa, representing an improvement. Furthermore, at a higher GNP content of 12 wt%, the modulus further increased to 41.2 MPa, exhibiting a remarkable 72.7% increment compared to the original TPS film. This demonstrates that the incorporation of GNP nanoparticles can greatly enhance the stiffness and mechanical properties of the biocomposites. The increased interfacial surface area of GNP nanoparticles allowed for better stress transmission and stiffening of the composites (King *et al.* 2013; Masarra *et al.* 2022).

However, it is important to note that an excessive content of GNP nanoparticles led to agglomeration and poor ductility of the material. The addition of 12 wt% and 15 wt% of GNP resulted in poor ductility, with elongation at break values of 2.58% and 1.33% respectively. This reduction in ductility can be attributed to the high aspect ratio and strong interaction of the stiff GNP filler with the polymer matrix. The presence of GNPs hindered the movement of polymer chains, leading to a deterioration in the mechanical behavior of the TPS. From the data tabulated in Table 3, it is clear that the tensile strength is dependent on the type of starch, the reinforcing material, and its weight percentage. The highest tensile strength was observed in potato starch with graphene oxide at 42 MPa, while the lowest was in corn/glycerol at 0.56 MPa. However, the Young's modulus in this work was comparable with previous studies. This suggests that there is a lot of room for optimization and further research in this field.

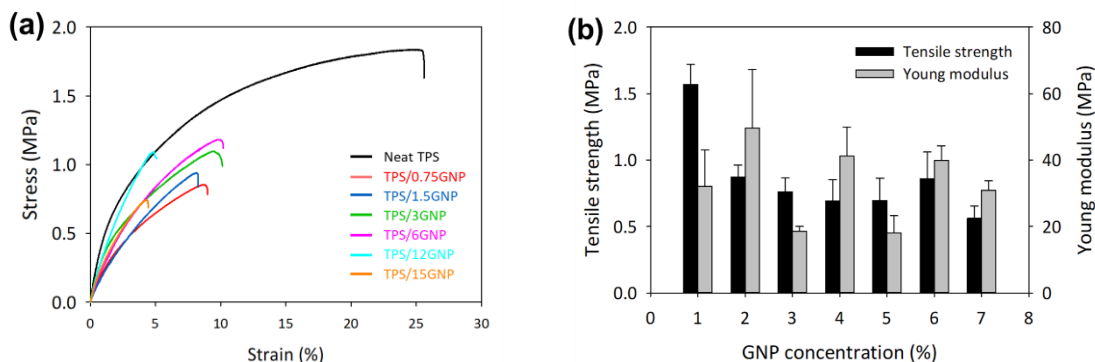


Fig. 5. (a) The stress-strain curves and (b) the trends of tensile strength and Young's modulus in TPS and TPS/GNP biocomposite films

Table 2. Mechanical Properties of the Biocomposite Films with Different GNP Concentrations

Film	Tensile Strength (MPa)	Tensile Strain (%)	Young's Modulus (MPa)
Neat TPS	1.57 ± 0.15	25.87 ± 1.13	32.12 ± 10.92
TPS/0.75GNP	0.87 ± 0.09	8.16 ± 0.59	49.59 ± 17.62
TPS/1.5GNP	0.76 ± 0.11	7.56 ± 0.50	18.44 ± 1.54
TPS/3GNP	0.69 ± 0.16	10.58 ± 2.17	41.20 ± 8.77
TPS/6GNP	0.70 ± 0.17	10.19 ± 0.64	17.99 ± 5.18
TPS/12GNP	0.86 ± 0.20	5.16 ± 0.86	39.92 ± 4.34
TPS/15GNP	0.56 ± 0.09	4.18 ± 0.18	30.90 ± 2.80

Table 3. Tensile Strength Comparison for Starch-Based Films Reinforced with Carbon Materials

Starch/Reinforced	Filler	Tensile Strength (MPa)	Young Modulus (MPa)	Reference
Sugar Palm /glycerol	12 wt% GNP	0.86	39.92	This study
Pea/ glycerol	2 wt% GO	13.79	1050	(Li <i>et al.</i> 2011)
Cassava/glycerol	10 wt% GO	1.6	189	(Zaki <i>et al.</i> 2021)
Potato/glycerol	1 wt% GO	42	47.3	(Islam and Mollik 2020)
Corn/glycerol	10.5 wt% carbon black	3.18	32.77	(Peidayesh <i>et al.</i> 2021)
Corn/glycerol/15% CNF	5 wt% GO nanoplatelets	0.56	29.6	(Ramezani <i>et al.</i> 2020)
Corn/glycerol/70% PVA	0.5 wt% Graphene nanosheets	10.4	53.33	(Jose <i>et al.</i> 2015)
Corn/glycerol/70% PVA	0.5 wt% CNT	7.34	66.04	(Jose <i>et al.</i> 2015)

Compatibility of Biocomposite Films

Figure 6(a) reveals the presence of voids or empty spaces within the starch granules in the TPS-based film. These voids are commonly observed because of the drying or

processing of the sample, leading to shrinkage and cracking of the granules, which weakens the film's strength.

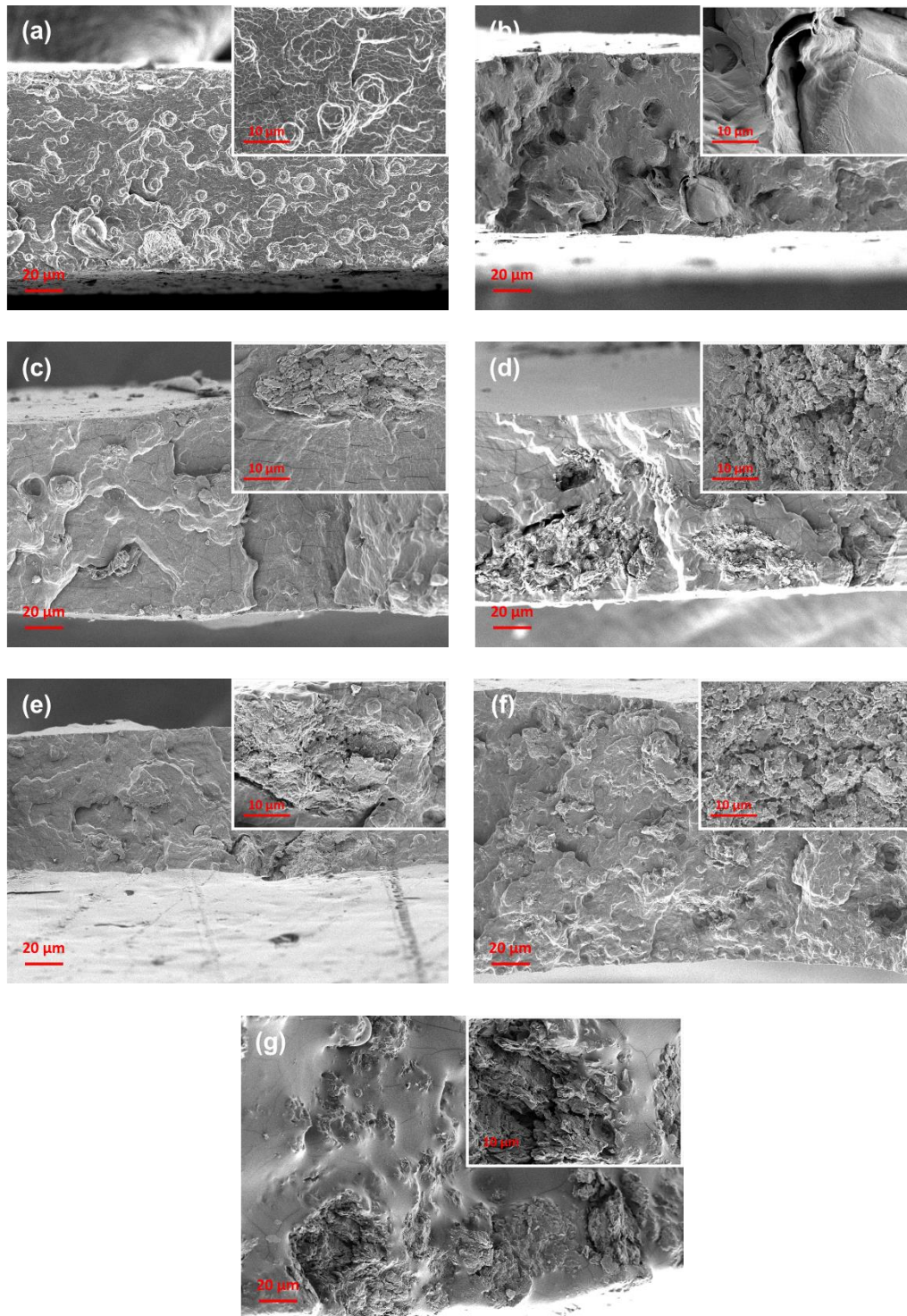


Fig. 6. FESEM tensile fracture surface morphology of (a) TPS, (b) TPS/0.75GNP, (c) TPS/1.5GNP, (d) TPS/3GNP, (e) TPS/6GNP, (f) TPS/12GNP, and (g) TPS/15GNP biocomposites film

Figure 6(b) demonstrates that starch and GNP can exhibit compatibility with each other. The GNP sheets were observed protruding from the impact fractured surface, indicating that the GNP nanoparticles were well-embedded and dispersed within the TPS matrix without any agglomeration. This uniform dispersion of GNP in the starch matrix is advantageous and can contribute to enhanced tensile strength of the composite material. The strong interaction between starch and GNP through hydrogen bonding and Van der Waals forces played a crucial role in maintaining this uniform dispersion.

However, when higher amounts of GNP were incorporated, particularly at 15 wt%, Fig. 6(g) illustrates a rougher film surface, poor dispersion of GNP, and the formation of GNP agglomerations. These agglomerations indicate that the GNP nanoparticles were no longer uniformly distributed within the starch matrix. This non-uniform dispersion and agglomeration of GNP can have detrimental effects on the mechanical properties of the composite material (Ibrahim *et al.* 2019).

CONCLUSIONS

In the frame of this work, starch-based nanocomposite filled with graphene nanoplatelets (GNP) were prepared *via* a solution casting method. The effects of GNP nanofillers on the physical, mechanical, and morphological properties of thermoplastic starch/GNP (TPS/GNP) composite films were investigated with different nanofiller contents of GNP. The following conclusions were drawn based on the extensive experimental study.

1. The results demonstrated that the addition of GNP nanoparticles effectively reduced the moisture absorption of TPS films due to the hydrophobic nature of graphene. The dispersion of GNP within the TPS matrix was influenced by the concentration of GNP, with 12 wt% of GNP showing the most uniform dispersion. The presence of GNP also led to an increase in the density and hydrophobicity of the films, as indicated by contact angle measurements.
2. Mechanical analysis revealed that the addition of GNP enhanced the tensile strength and Young's modulus of the TPS/12GNP leading to the highest improvement. However, excessive TPS/15GNP resulted in poor ductility and decreased tensile strength, highlighting the importance of optimizing the GNP concentration for desired mechanical properties.
3. The study demonstrated that GNP can be effectively used as nanofillers to improve the Young's modulus and barrier properties of thermoplastic sugar palm starch films. These modified biocomposites have potential applications in various fields, including intelligent food packaging, biomedical devices, and environmentally friendly electronics, contributing to the development of sustainable and eco-friendly materials for future technologies. Further research could focus on optimizing the GNP concentration and exploring additional processing techniques to enhance the overall performance of these biocomposites.

ACKNOWLEDGMENTS

The authors are grateful for the support of the Universiti Kebangsaan Malaysia, Grant No. GUP-2021-018.

REFERENCES CITED

- Ahmad, Z., Hermain, H. Y., and Abdul Razak, N. H. (2015). "Mechanical and physical properties of sago starch/halloysite nanocomposite film," *Advanced Materials Research* 1115, 394-397. DOI: 10.4028/www.scientific.net/amr.1115.394
- Arpitha, G. R., Verma, A., Sanjay, M. R., Gorbatyuk, S., Khan, A., Sobahi, T. R., Asiri, M. A., and Siengchin, S. (2022). "Bio-composite film from corn starch based vetiver cellulose," *Journal of Natural Fibers* 19(16), 14634-14644. DOI: 10.1080/15440478.2022.2068174
- ASTM D570-98 (1998). "Standard test methods for water absorption of plastics," ASTM International, West Conshohocken, PA, USA.
- ASTM D792-00 (2000). "Standard test method for density and specific gravity (relative density) of plastic by displacement," ASTM International, West Conshohocken, PA, USA.
- Cataldi, P., Athanassiou, A., and Bayer, I. S. (2018). "Graphene nanoplatelets-based advanced materials and recent progress in sustainable applications," *Applied Sciences (Switzerland)* 8(9), article 1438. DOI: 10.3390/app8091438
- Chen, Y., Guo, Z., Das, R., and Jiang, Q. (2020). "Starch-based carbon nanotubes and graphene: Preparation, properties and applications," *ES Food & Agroforestry* 13-21. DOI: 10.30919/esfaf1111
- Cheng, H., Chen, L., McClements, D. J., Yang, T., Zhang, Z., Ren, F., Miao, M., Tian, Y., and Jin, Z. (2021). "Starch-based biodegradable packaging materials: A review of their preparation, characterization and diverse applications in the food industry," *Trends in Food Science and Technology* 114(February), 70-82. DOI: 10.1016/j.tifs.2021.05.017
- Chia, M. R., Phang, S. W., and Ahmad, I. (2023). "Influence of polyaniline and cellulose nanocrystals on starch biopolymer film for intelligent food packaging," *Food Bioscience* 56, article ID 103212. DOI: 10.1016/j.fbio.2023.103212
- Bumrungnok, K., Threepopnatkul, P., Amornsakchai, T., Chia, C. H., Wongsagonsup, R., and Smith, S. M. (2023). "Toward a circular bioeconomy: Exploring pineapple stem starch film as protective coating for fruits and vegetables," *Polymers* 15(11), article ID 2493. DOI: 10.3390/polym15112493
- Dong, W., Li, W., Zhu, X., Sheng, D., and Shah, S. P. (2021). "Multifunctional cementitious composites with integrated self-sensing and hydrophobic capacities toward smart structural health monitoring," *Cement and Concrete Composites* 118(January), article ID 103962. DOI: 10.1016/j.cemconcomp.2021.103962
- Feng, J., Safaei, B., Qin, Z., and Chu, F. (2023). "Nature-inspired energy dissipation sandwich composites reinforced with high-friction graphene," *Composites Science and Technology* 233, article ID 109925. DOI: 10.1016/j.compscitech.2023.109925
- George, A., Sanjay, M. R., Srisuk, R., Parameswaranpillai, J., and Siengchin, S. (2020). "A comprehensive review on chemical properties and applications of biopolymers

- and their composites,” *International Journal of Biological Macromolecules* 154, 329-338. DOI: 10.1016/j.ijbiomac.2020.03.120
- Gutiérrez, T. J., Ollier, R., and Alvarez, V. A. (2018). “Surface properties of thermoplastic starch materials reinforced with natural fillers,” *Springer Series on Polymer and Composite Materials* 131-158. DOI: 10.1007/978-3-319-66417-0_5
- Ibrahim, F., Mohan, D., Sajab, M. S., Bakarudin, S. B., and Kaco, H. (2019). “Evaluation of the compatibility of organosolv lignin-graphene nanoplatelets with photo-curable polyurethane in stereolithography 3D printing,” *Polymers* 11(10), article ID 1544. DOI: 10.3390/polym11101544
- Islam, M. R., and Mollik, S. I. (2020). “Enhanced electrochemical performance of flexible and eco-friendly starch/graphene oxide nanocomposite,” *Heliyon* 6(10), article ID e05292. DOI: 10.1016/j.heliyon.2020.e05292
- Jose, J., Al-Harhi, M. A., AlMa’adeed, M. A. A., Dakua, J. B., and De, S. K. (2015). “Effect of graphene loading on thermomechanical properties of poly(vinyl alcohol)/starch blend,” *Journal of Applied Polymer Science* 132(16), Article Number 41827. DOI: 10.1002/app.41827
- Jose, J., De, S. K., Ma’adeed, M. A. A. Al, Bhadra Dakua, J., Sreekumar, P. A., Sougrat, R., and Al-Harhi, M. A. (2015). “Compatibilizing role of carbon nanotubes in poly(vinyl alcohol)/starch blend,” *Starch/Staerke* 67(1–2), 147-153. DOI: 10.1002/star.201400074
- Kabir, H., and Garg, N. (2023). “Machine learning enabled orthogonal camera goniometry for accurate and robust contact angle measurements,” *Scientific Reports* 13(1), 1-13. DOI: 10.1038/s41598-023-28763-1
- Khalid, N. N., Mohd Radzuan, N. A., Sulong, A. B., Mohd Foudzi, F., and Gunasegran, M. (2022). “Simulation analysis of graphene addition on polymeric composite,” *Jurnal Kejuruteraan* 34(5), 941-947. DOI: 10.17576/jkukm-2022-34(5)-22
- Kim, E., Kim, D., Kwak, K., Nagata, Y., Bonn, M., and Cho, M. (2022). “Wettability of graphene, water contact angle, and interfacial water structure,” *Chem* 8(5), 1187-1200. DOI: 10.1016/j.chempr.2022.04.002
- King, J. A., Klimek, D. R., Miskioglu, I., and Odegard, G. M. (2013). “Mechanical properties of graphene nanoplatelet/epoxy composites,” *Journal of Applied Polymer Science* 128(6), 4217-4223. DOI: 10.1002/app.38645
- Kiziltas, A., Liu, W., Tamrakar, S., and Mielewski, D. (2021). “Graphene nanoplatelet reinforcement for thermal and mechanical properties enhancement of bio-based polyamide 6, 10 nanocomposites for automotive applications,” *Composites Part C: Open Access* 6, article ID 100177. DOI: 10.1016/j.jcomc.2021.100177
- Li, R., Liu, C., and Ma, J. (2011). “Studies on the properties of graphene oxide-reinforced starch biocomposites,” *Carbohydrate Polymers* 84(1), 631-637. DOI: 10.1016/j.carbpol.2010.12.041
- Masarra, N. A., Batistella, M., Quantin, J. C., Regazzi, A., Pucci, M. F., Hage, R. El, and Lopez-Cuesta, J. M. (2022). “Fabrication of PLA/PCL/graphene nanoplatelet (GNP) electrically conductive circuit using the fused filament fabrication (FFF) 3D printing technique,” *Materials* 15(3), article 762. DOI: 10.3390/ma15030762
- Mergen, Ö. B., Arda, E., and Evingür, G. A. (2020). “Electrical, optical and mechanical properties of chitosan biocomposites,” *Journal of Composite Materials* 54(11), 1497-1510. DOI: 10.1177/0021998319883916
- Mohan, D., Bakir, A. N., Sajab, M. S., Bakarudin, S. B., Mansor, N. N., Roslan, R., and Kaco, H. (2021a). “Homogeneous distribution of lignin/graphene fillers with

- enhanced interlayer adhesion for 3D printing filament,” *Polymer Composites* 42(5), 2408-2421. DOI: 10.1002/pc.25987
- Mohan, D., Khai, T. Z., Sajab, M. S., and Kaco, H. (2021b). “Well-dispersed cellulose-graphene in 4D printing biopolymer,” *Materials Letters* 303, article ID 130522. DOI: 10.1016/j.matlet.2021.130522
- Muthukumar, C., Krishnasamy, S., Thiagamani, S. M. K., and Siengchin, S. (2022). *Aging Effects on Natural Fiber-Reinforced Polymer Composites*, Springer, Singapore. DOI: 10.1007/978-981-16-8360-2
- Namdev, A., Telang, A., and Purohit, R. (2023). “Water absorption and thickness swelling behaviour of graphene nanoplatelets reinforced epoxy composites,” *International Journal of Advanced Technology and Engineering Exploration* 10(98), 120-127. DOI: 10.19101/IJATEE.2021.874756
- Otálora González, C. M., Flores, S. K., Basanta, M. F., and Gerschenson, L. N. (2020). “Effect of beetroot (*Beta vulgaris* L. var *conditiva*) fiber filler and corona treatment on cassava starch films properties,” *Food Packaging and Shelf Life* 26(November). DOI: 10.1016/j.fpsl.2020.100605
- Papadopoulou, E. L., Pignatelli, F., Marras, S., Marini, L., Davis, A., Athanassiou, A., and Bayer, I. S. (2016). “Nylon 6,6/graphene nanoplatelet composite films obtained from a new solvent,” *RSC Advances* 6(8), 6823-6831. DOI: 10.1039/c5ra23647a
- Peidayesh, H., Mosnáčková, K., Špitalský, Z., Heydari, A., Šišková, A. O., and Chodák, I. (2021). “Thermoplastic starch-based composite reinforced by conductive filler networks: Physical properties and electrical conductivity changes during cyclic deformation,” *Polymers* 13(21), article ID 3819. DOI: 10.3390/polym13213819
- Ramezani, H., Behzad, T., and Bagheri, R. (2020). “Synergistic effect of graphene oxide nanoplatelets and cellulose nanofibers on mechanical, thermal, and barrier properties of thermoplastic starch,” *Polymers for Advanced Technologies* 31(3), 553-565. DOI: 10.1002/pat.4796
- Scaffaro, R., Botta, L., Maio, A., and Gallo, G. (2017). “PLA graphene nanoplatelets nanocomposites: Physical properties and release kinetics of an antimicrobial agent,” *Composites Part B: Engineering* 109, 138-146. DOI: 10.1016/j.compositesb.2016.10.058
- Shahbazi, M., Rajabzadeh, G., and Sotoodeh, S. (2017). “Functional characteristics, wettability properties and cytotoxic effect of starch film incorporated with multi-walled and hydroxylated multi-walled carbon nanotubes,” *International Journal of Biological Macromolecules* 104, 597-605. DOI: 10.1016/j.ijbiomac.2017.06.031
- Tarhini, A. A., and Tehrani-Bagha, A. R. (2019). “Graphene-based polymer composite films with enhanced mechanical properties and ultra-high in-plane thermal conductivity,” *Composites Science and Technology* 184, article ID 107797. DOI: 10.1016/j.compscitech.2019.107797
- Vinod, A., Sanjay, M. R., Suchart, S., and Jyotishkumar, P. (2020). “Renewable and sustainable biobased materials: An assessment on biofibers, biofilms, biopolymers and biocomposites,” *Journal of Cleaner Production* 258, article ID 120978. DOI: 10.1016/j.jclepro.2020.120978
- Yemenicioğlu, A., Farris, S., Turkyilmaz, M., and Gulec, S. (2020). “A review of current and future food applications of natural hydrocolloids,” *International Journal of Food Science and Technology* 55(4), 1389-1406. DOI: 10.1111/ijfs.14363

Zaki, N. N. M., Yunin, M. Y. A. M., Adenam, N. M., Noor, A. M., Wong, K. N. S. W. S., Yusoff, N., and Adli, H. K. (2021). "Physicochemical analysis of graphene oxide-reinforced cassava starch biocomposites," *Biointerface Research in Applied Chemistry* 11(5), 13232-13243. DOI: 10.33263/BRIAC115.1323213243

Article submitted: November 7, 2023; Peer review completed: December 9, 2023;
Revised version received: December 25, 2023; Accepted: January 1, 2024; Published:
January 16, 2024.

DOI: 10.15376/biores.19.1.1526-1541